Hindawi
Advances in Civil Engineering
Volume 2024, Article ID 6681592, 9 pages
https://doi.org/10.1155/2024/6681592

*Research Article*

# Experimental Study of Macro- and Micro-Scopic Damage in Red Sandstone under Dry and Wet Cycling

**Xiangmei Chen,[1,2] Yongqiang Ren,[1] Baoli Tang,[1] Guojin Li,[1] Feitian Zhang,[1] and Yunfei Liu[1]**

[1]*Department of Civil Engineering, Ordos Institute of Technology, Ordos 017000, China*
[2]*School of Chemical Engineering, The Inner Mongolia University of Technology, Hohhot 010051, China*

Correspondence should be addressed to Yongqiang Ren; ryongqiang@oit.edu.cn

Received 27 June 2023; Revised 3 April 2024; Accepted 10 April 2024; Published 23 April 2024

Academic Editor: Zengping Zhang



The high-strength red sandstone in its natural state is subjected to significant strength deterioration under alternating wet and dry conditions, which can cause many catastrophic problems in the process of engineering construction. It is important to deeply understand the damage mechanism of red sandstone under the action of dry and wet cycles. Therefore, this paper explores the mechanism of red sandstone's uniaxial deformation and failure through indoor uniaxial compression tests, studies the damage to the microstructure of red sandstone under wet–dry cycles using scanning electron microscopy, and establishes a damage variable based on fractal dimension. The results show that with the increase of wet–dry cycles, the peak stress of red sandstone shows a decreasing trend, and the minimum peak stress is 17.3 MPa, which is a 46.62% decrease compared to the sample with 0 wet–dry cycles. During the wet–dry cycle process, there are four deformation characteristics of red sandstone samples, namely, crack compression, crack extension, progressive fracture, and crack penetration. SEM images show that the porosity, pore area, and fractal dimension all show a nonlinear increase, and the maximum damage variable can reach 10.41%. The research results can provide guidance for engineering design and slope failure mechanism research in red sandstone areas.

## 1. Introduction

In recent years, the Ordos region has experienced frequent extreme rainfall events, leading to high levels of rainfall and temperatures during the summer months. This can cause rocks to undergo periodic wet and dry cycles, which can result in the deterioration of their physical and mechanical properties [1–6]. This poses significant challenges for geotechnical construction in the region. Therefore, studying the macroscopic and microscopic damage degradation laws of red sandstone under dry–wet cycling environment is of great significance for guiding the construction of geotechnical engineering in the Ordos region and other red sandstone areas.

Previous studies have extensively investigated the dry and wet cycling processes of red sandstone, which causes structural softening and strength loss. Zhou et al. [7, 8] proposed that irreversible cumulative fracture damage under wet and dry cycle treatment is the main cause of strength reduction in sandstone. Zhang et al. [9] used acoustic emission techniques to study the damage characteristics of sandstone under the action of dry and wet cycles and found that the uniaxial compressive strength and modulus of elasticity increase with the number of wet and dry cycles. Du et al. [10] showed that dry and wet cycles have a significant degrading effect on dynamic fracture properties. Yao et al. [11] demonstrated that during the dry–wet cycle, water–rock interactions lead to progressive changes in mineral composition, microstructure, and micropores. Khanlari and Abdilor [12] studied the effect of dry–wet, freeze–thaw, and hot–cool cycles on the physical and mechanical properties of the upper red sandstone in Central Iran. Ying et al. [13] suggested that the number of wet and dry cycles has an effect on type I crack extension, with the fracture toughness decreasing and dispersing as the number of cycles increases. The crack expansion speed is accelerated, and the crack initiation time is shortened. Cai et al. [14] found that the fracture toughness and energy dissipation of sandstone decreased

Table 1: Main physical and hydraulic properties parameters of rock samples.

| Formation lithology | Natural density, $\rho$ (g/cm$^3$) | Dry density, $\rho_d$ (g/cm$^3$) | Saturated density, $\rho_w$ (g/cm$^3$) | Saturated water absorption, $W_{sa}$ (%) | Natural water absorption, $W_a$ (%) | Natural moisture content, $W$ (%) | Saturation coefficient, $K_s$ |
|---|---|---|---|---|---|---|---|
| Purple-red sandstone | 2.34 | 2.32 | 2.43 | 3.85 | 2.47 | 0.61 | 0.64 |

significantly with the increase in the number of cycles, and the interparticle calcite cement gradually dissolved after cyclic wet and dry treatment. The above studies show that dry and wet cycling will deteriorate the mechanical properties of red sandstone, but their research tools mainly utilize mechanical and physical indicators and indicators such as microscopic pores, without in-depth study of pore parameters (e.g., fractal dimensions [15–21]), and lack of research on microscopic damage variables of red sandstone.

And the wet and dry cycles will not only affect the mechanical property changes of red sandstone but also cause damage to the red sandstone soil. Currently, Chen et al. [22] analyzed the effect of water content and fracture angle on rock strength, damage mode, and acoustic emission properties. In particular, kernel density estimation (KDE) was used to quantify the spatial distribution of acoustic emission events and to distinguish the difference in damage patterns between dry and saturated rocks. Studies have shown that the presence of water in the rock reduces the strength of the rock. The number and acoustic emission count of secondary cracks are reduced. With the increase of fracture angle, the rock strength and acoustic emission number increase, and the damage mode changes from tensile damage to shear damage [23]. However, this study did not consider the impact of dry–wet cycles on red sandstone and lacked the effect of dry–wet cycles on fracture angle. Therefore, the conclusions drawn did not fully explain the failure mode of red sandstone [24]. Further damage modeling is also needed to elucidate the degradation mechanism of red sandstone under dry and wet cycling.

In summary, wet and dry cycles have significant effects on rock deterioration, and previous studies have mainly reflected the deterioration of rocks by dry and wet cycles through changes in physical and mechanical properties. However, the deterioration mechanism of red sandstone under dry and wet cycles from damage mechanics and microscopic perspectives is lacking. The damage deterioration pattern of red sandstone is rarely studied, and the corresponding damage variables need to be studied.

Therefore, this study aims to use Ordos red sandstone as the research object to conduct uniaxial compression and microscopic tests on red sandstone with different numbers of wet and dry cycles. The response law of physical parameters such as stress–strain curve, strength loss [25, 26], porosity, pore area, and fractal dimension of red sandstone to the number of dry and wet cycles will be studied. This will reveal the mechanism of macro- and micro-deformation damage deterioration of red sandstone under dry and wet cycles. Finally, the fractal dimension will be used to define the damage of red sandstone after dry and wet cycles, and the damage variables of dry and wet cycle red sandstone will be defined.

Figure 1: Photos of sampling points.

The research results can provide a reference basis for the deformation, damage, and deterioration of red sandstone under dry and wet conditions.

## 2. Materials and Methods

*2.1. Basic Physical and Mechanical Properties of Red Sandstone.* In accordance with the "Standard Test Methods for Engineering Rock Masses" (GB/T 50266-2013), laboratory testing was conducted to determine the basic physical properties of red sandstone. The results of the tests are presented in Table 1. Statistical analysis of the data in Table 1 reveals that the water saturation coefficient of red sandstone in the Ordos region is relatively high. Rock formations containing clay minerals have limited space for clay expansion after water absorption, which can lead to swelling and fragmentation, resulting in a significant decrease in rock strength [27].

Moreover, X-ray diffraction was employed to analyze the mineral composition of the red sandstone. The analysis revealed that the clay mineral components of the red sandstone are montmorillonite, chlorite, illite, and kaolinite, with a high clay mineral content of over 64%. The detrital components are mainly composed of quartz, calcite, and feldspar.

*2.2. Red Sandstone Sample Preparation.* The red sandstone used in this article was selected from the red sandstone in the Ordos region (as shown in Figure 1), with a purple-red appearance and an average density of 23.40 kN/m$^3$. Cubic sandstone blocks were cut on-site and transported to the rock mechanics laboratory for processing [28]. In accordance with the requirements of rock mechanics testing standards, the processed samples had an average size of 50.00 mm × 100 mm. To ensure the smooth completion of the experiment, a total of 60 cylindrical samples were prepared. In order to avoid discontinuity in the test results, each group of samples was

subjected to three dry and wet cycle tests, and the experimental results were averaged.

*2.3. Dry and Wet Cycle Test Design and Method.* According to the "Highway Geotechnical Test Procedure" (JTG E40-2007), the drying temperature for rock in the standard state is 105°C. In this state, the free and bound water of the rock will be completely dissipated [29]. However, considering that the destabilization of the slopes in this area mostly occurs in summer and the surface temperature can only reach a maximum of 60–70°C. At the same time, most structural damage is caused by the formation of cracks due to the dissipation of free water from the rock structure. Therefore, the dry and wet cycle test is designed to simulate the rock surface temperature conditions under natural conditions, so the drying temperature is 70°C. The drying state was selected as the initial cycle state and the saturated state as the cycle termination state for this test [30]. The test is carried out in five groups of three specimens each at 0, 5, 10, 15, and 25 cycles for uniaxial compression tests. One of the dry and wet cycle processes consists of two parts: extraction saturation and drying [31].

To begin the process, place the specimen in the oven, turn on the dehumidifying and drying fan, and dry at 70°C for 12 hr to determine the quality of the specimen. The process of pumping saturated air is as follows: The specimen is placed in the vacuum saturation device and evacuated until the pressure gauge reads close to 0.1 MPa (1 standard atmospheric pressure). Allow the value to stabilize before continuing to pump for about 4 hr, then place the pumping tube into the water tank. Open the suction valve and slowly pump the water into the vacuum saturator. When the water surface exceeds the height of the specimen, lift the water pipe from the sink. The specimen is allowed to stand at atmospheric pressure for 12 hr and then removed. At this point, the test piece has finished absorbing water. Remove and dip the surface water and weigh. Drying and pumping saturated once for one cycle. Measure the longitudinal wave velocity and dimensions of the rock sample after each cycle [32].

*2.4. Uniaxial Compression Test Method.* The uniaxial compression test of red sandstone was conducted using a new Changchun tester (TSW-1000). The tester is produced by Changchun New Testing Machine Co., Ltd., and has a maximum axial force of 2,000 kN and a maximum circumferential pressure of 100 MPa. It can conduct routine unconfined compression tests and triaxial compression tests. To avoid any discreteness in the test results, the average of three samples completed in each group of tests is taken. During the experiment, displacement control was used, with a loading rate of 0.02 mm/s, until the sample was damaged, and pressure was relieved [33].

In summary, the red sandstone samples were prepared and tested using a dry and wet cycle test and uniaxial compression test method. The test results will provide valuable insights into the mechanical properties of red sandstone and its potential for use in slope stabilization.

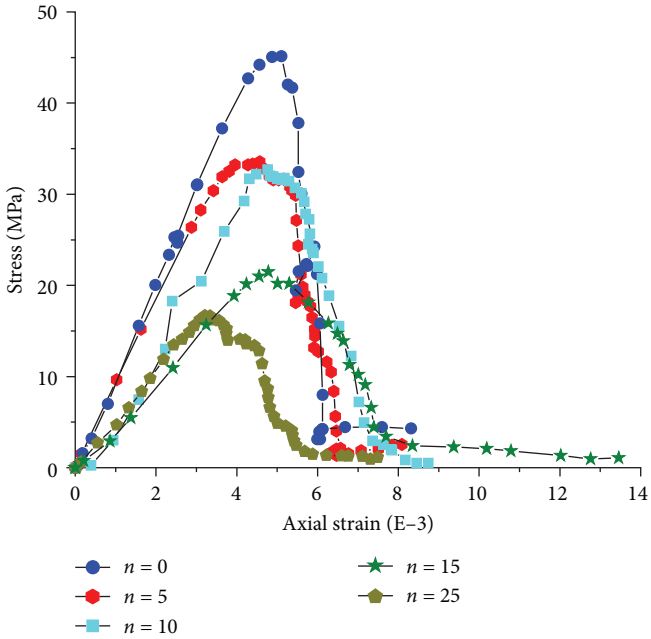


FIGURE 2: Stress–strain curve ($n$ is the number of wet and dry cycles).

## 3. Analysis of Test Results

*3.1. Stress–Strain Curve.* In order to investigate the damage characteristics of red sandstone under uniaxial compression by dry and wet cycles, a study was conducted. The unconfined compressive strength test was carried out, and the stress–strain curve of the specimen was plotted for different numbers of wet and dry cycles (Figure 2). The stress–strain curves exhibited a single-peak shape at varying numbers of wet and dry cycles. At $n = 0$, the peak stress in the red sandstone was 32.41 MPa. However, as the number of wet and dry cycles increased, the peak stress tended to decrease nonlinearly. At $n = 5$, the peak stress reached 31.95 MPa, which was a decrease of 1.44% from 0 cycles of wet and dry. At $n = 10$, the peak stress decreased even further to 27.90 MPa. This was due to the fact that the higher the number of wet and dry cycles, the more fissures were induced in the red sandstone, causing serious damage to its internal structure and resulting in a decrease in its strength index. The peak stresses were 27.05 and 17.30 MPa for $n = 15$ and 20, respectively. This indicates that with increasing numbers of wet and dry cycles, there was already a large amount of primary fracturing within the red sandstone. After the immersion process, water penetrated into the interior of the red sandstone and entered the fracture tip microfracture damage zone of water to form cleavage. The water pressure acting on the surface of the microfracture increased the stress intensity factor at the tip of the fracture, prompting the microfracture within the red sandstone to crack and extend, increasing the porosity of the red sandstone and expanding its volume. This led to the progressive development of primary microfractures under the influence of water damage and the generation of new secondary fractures, causing irreversible progressive damage to the red sandstone. Therefore, the higher the number of

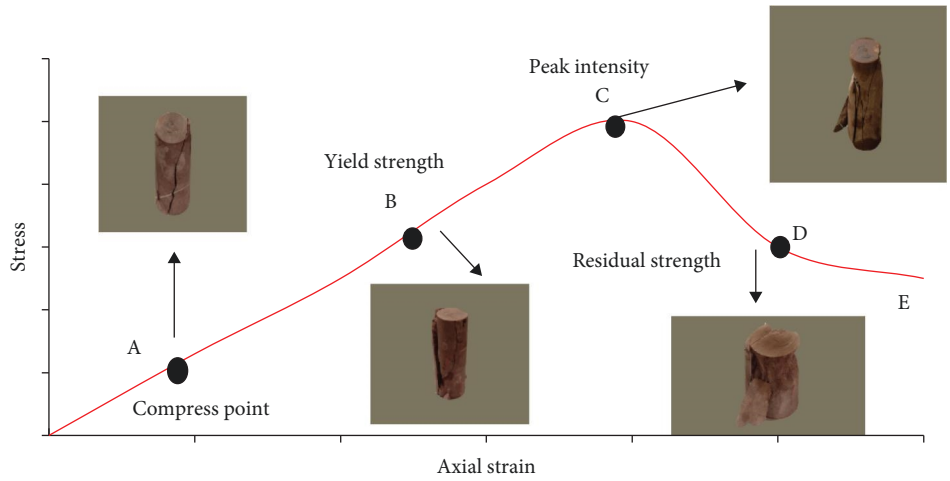


Figure 3: Stress–strain curve model.

wet and dry cycles, the more pore space within the red sandstone, further leading to a decrease in peak stress in the red sandstone specimen.

It is also observed that the stress–strain curve shows a sawtooth shape after the peak stress for 0, 5, and 15 cycles of wet and dry conditions. The reason for this is the heterogeneous nature of the red sandstone itself and the random development of initial and secondary cracks and development of cracks under "wet–dry" damage. The combination of uniaxial loading and dry–wet alternation has resulted in a rock failure mode based on "dry–wet" interaction. This causes the complexity of existing newly created cracks to deepen, as evidenced by increased undulations and fluctuations in the stress–strain curve. The internal fractures in the red sandstone also produce more undulating ripples, with a significant increase in the distribution interval of mechanical parameters such as stress and strain, and a jagged curve over a range.

*3.2. Characterization of Uniaxial Deformation of Rocks by Dry and Wet Cycles.* Based on the stress–strain curve presented in Figure 2, the stress–strain behavior of red sandstone subjected to wet and dry cycles can be represented by the complete process model of red sandstone deformation, as shown in Figure 3. The wet and dry cycles induce four distinct stages of fracture evolution, including the compression, extension, progression, and penetration stages.

(1) Section OB is a fracture compacted section. The main components are the OA section of the compression dense zone and the AB section of the elastic zone. Compressive closure of primary microcracks due to the application of axial loads. It was also found that the fracture closure stress $\sigma_{cc}$ at the end of the OA stage was about 10%–20% of the peak stress $\sigma_c$. After fracture compression, the rock is transformed from a discontinuous medium to a seemingly continuous medium and enters the elastic deformation stage AB section. AB ends with an initial crack initiation stress $\sigma_{ci}$ of approximately 30%–50% of the peak stress $\sigma_c$.

(2) Section BC is a fissure extension. When the elastic limit is exceeded, microfractures in the rock begin to develop, expand, and accumulate. Fractures within the rock develop as the stress difference increases. When the crack initiation stress is reached, the originally compacted and closed fractures begin to continue to expand and new cracks will appear between some of the relatively weaker grain boundaries.

(3) Segment CD is a rupture progression segment. Upon entering this phase, a qualitative change in the development of microfractures occurs. Due to the significant stress concentration effect caused by the rupture process, the rupture will continue to develop progressively even if the working stress remains constant. After the rock has reached its peak strength, strain softening occurs as the strain increases and the stress continues to decrease.

(4) Section DE is a fissure through section. Development of microfracture surfaces within the rock mass into through fracture surfaces. Rapid loss of strength of the rock mass but continued growth of plastic deformation.

*3.3. Uniaxial Strength Loss Pattern in Red Sandstone.* In order to explore the impact of wet–dry cycles on the mechanical properties of red sandstone, this study aims to define the rate of strength loss ($W_j$) and deformation ($E_j$) of red sandstone under different wet–dry cycle numbers (0 cycles and beyond). Equations (1) and (2) will be utilized to calculate $W_j$ and $E_j$, respectively:

$$W_j = \frac{\sigma_j - \sigma_0}{\sigma_0} \times 100\%, \tag{1}$$

$$E_j = \frac{E_j - E_0}{E_0} \times 100\%. \tag{2}$$

The data in Table 2 were analyzed to determine the average values of uniaxial compressive strength ($\sigma_c$) and modulus of elasticity ($E$). These values were obtained before ($\sigma_j$) and

Table 2: Deterioration analysis of uniaxial compression strength parameters of red sandstone.

| Cycle stage ($i$) | Number of cycles ($N$) | Uniaxial compressive strength, $\sigma_c$ (MPa) | Total loss of compressive strength in wet and dry cycles, $W_j = \frac{\sigma_j - \sigma_0}{\sigma_0} \times 100\%$ (*Phase i-1 loss ratio*) | Elastic modulus, $E$ (GPa) | Total loss of modulus of elasticity in dry and wet cycles, $E_j = \frac{E_j - E_0}{E_0} \times 100\%$ (*Phase i-1 loss ratio*) |
|---|---|---|---|---|---|
| I | 0 | 32.41 | 0 | 9.2 | 0 |
| II | 5 | 31.95 | 1.41 (1.41) | 9.3 | 1.08 (1.08) |
| III | 10 | 27.90 | 13.91 (12.50) | 7.45 | 20.82 (19.75) |
| IV | 15 | 27.05 | 16.53 (2.61) | 7.51 | 20.10 (−0.71) |
| V | 25 | 17.30 | 46.62 (30.09) | 4.77 | 49.24 (29.13) |

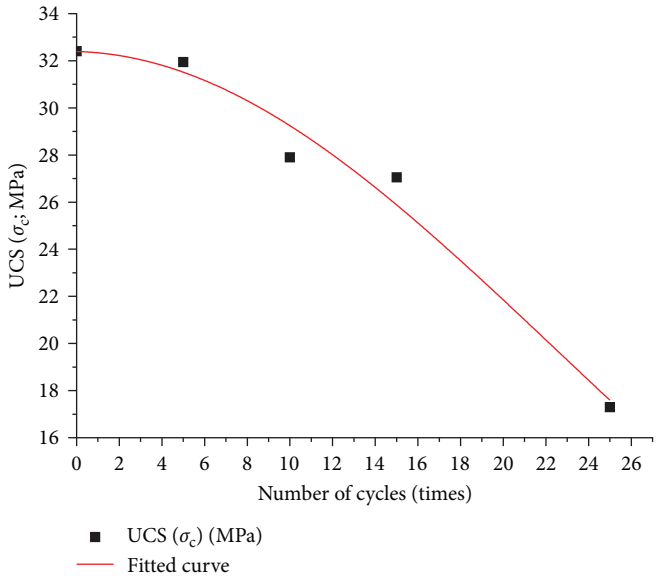


Figure 4: Average uniaxial compressive strength versus number of wet and dry cycles.

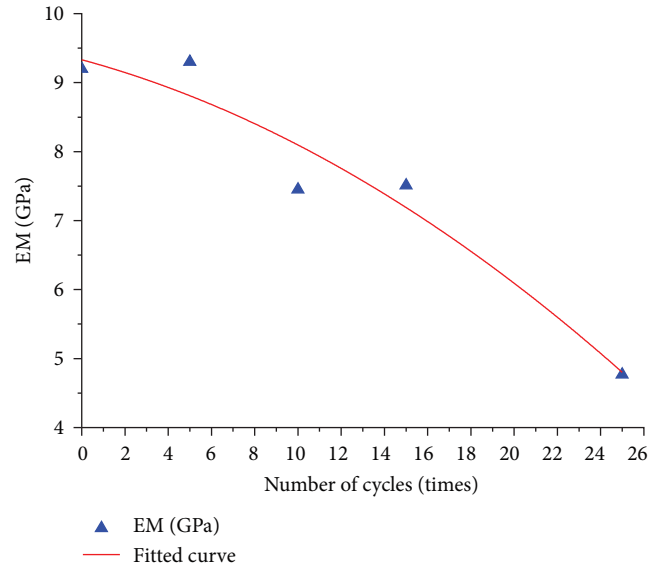


Figure 5: Average modulus of elasticity versus number of wet and dry cycles.

after ($\sigma_0$) the initial cycle, as well as after subsequent cycles ($E_j$). Additionally, the initial cyclic mean modulus of elasticity ($E_0$) was also considered. The results of this analysis are presented in Figures 4 and 5.

Table 2 and Figures 4 and 5 reveal that the red sandstone's uniaxial compressive strength and modulus of elasticity decrease as the number of wet and dry cycles increases. The impact of wet and dry cycles on Poisson's ratio is negligible. The total loss rate of strength and deformation indices of the red sandstone increases throughout all stages as the number of wet and dry cycles increases. However, the initial stage shows insignificant strength depreciation. The uniaxial compressive strength $\sigma_c$ only decreases by 1.41%, and the modulus of elasticity $E$ by 1.08%, which is consistent with the rock's preabsorption pattern. As the number of wet and dry cycles (25) increases, the rate of loss of uniaxial compressive strength $\sigma_c$ reaches 46.62%, and the rate of loss of modulus of elasticity $E$ reaches 49.24%. This indicates the progressive deterioration of the rock by water during the wet and dry cycles. Additionally, the rate of loss of strength deformation in stages III and IV is demonstrated by the compressive strength $\sigma_c$ being less than the modulus of elasticity $E$. This also suggests that water has a more significant impact on the rock's deformation parameters during the wet and dry cycles.

The correlation analysis between $\sigma_c$, $E$, and the number of dry and wet cycles $n$ indicates a strong negative exponential relationship with $n$. As shown in Figure 6, the trend of uniaxial compressive strength and modulus of elasticity reveals a relatively stable reduction until 15 wet and dry cycles for red sandstone. However, beyond 15 cycles, the uniaxial compressive strength of red sandstone experiences a significant decline, accompanied by an increased reduction rate of the modulus of elasticity. These findings suggest that the strength of red sandstone deteriorates progressively under various wet and dry cyclic conditions, leading to the accelerated development of pores and fissures within the rock.

*3.4. Microanalysis.* In order to investigate the damage mechanism of red sandstone caused by dry and wet cycles, we utilized SEM images to analyze the microstructural changes of red sandstone from a microscopic perspective under different dry and wet cycles. Figure 7 shows the SEM image. At 0 cycles, the red sandstone grains are closely aligned and there are no large pores. However, as the number of cycles

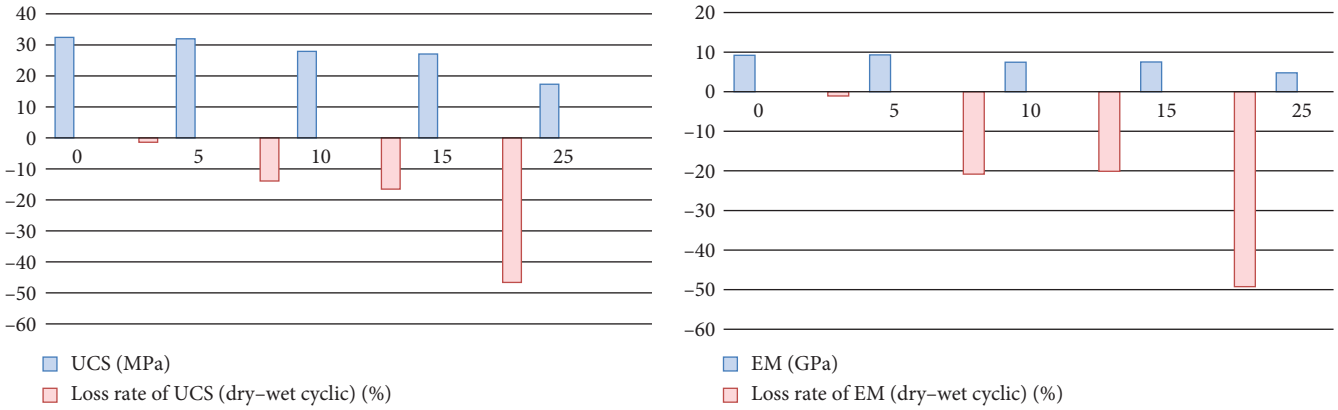


Figure 6: Rock strength and deformation loss rate under wet and dry cycles.

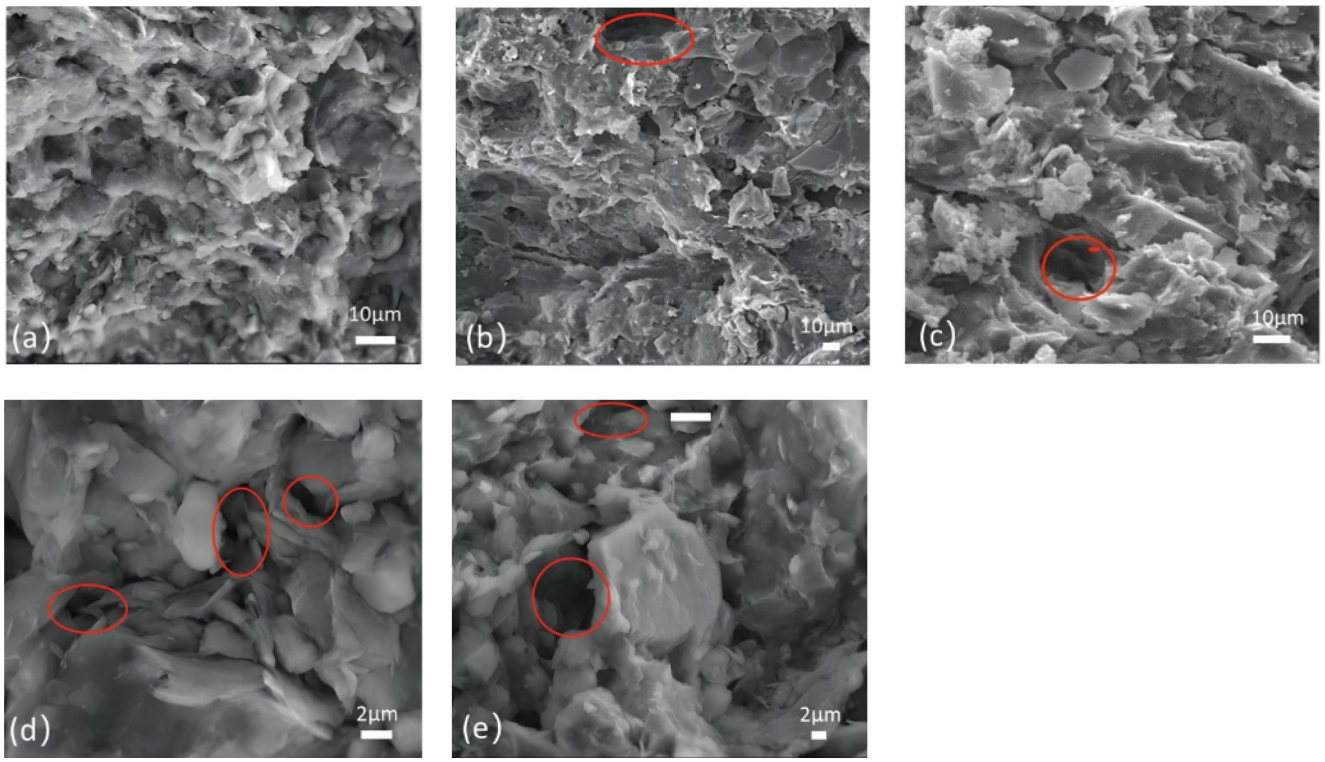


Figure 7: SEM images for the surfaces of red sandstone after different dry–wet cycle number: (a) $n = 0$; (b) $n = 5$; (c) $n = 10$; (d) $n = 15$; and (e) $n = 25$.

increases (5 and 10), the red sandstone grains become loosely aligned and pore space is developed, with visible large pores. The minerals are mostly rounded and free from angularity, with flocculated secondary mineral aggregates developing on the surface and alteration of the remaining darker minerals. The microscopic results after wet and dry cycling correspond to the mechanical parameters of the specimens. With the increase in the number of wet and dry cycles, the clay minerals inside the sandstone specimens gradually decreased, the cementation force between the particles decreased, the internal pores increased, the microcracks increased, and the macroscopic results showed that the mechanical properties decreased. At 15 and 25 cycles, the structure of the red sandstone is dominated by individual mineral grains and mineral aggregates (agglomerates), with loosely arranged grains, well-developed fissures, and large pores that are easily compressed. Various clay minerals are stacked or agglomerated in sheets or coils, with slight alteration at the edges. And it can be observed that after the dry and wet cycles, the horizontal section appears interparticle pores and intraparticle pores, the structure is loose and bulging, and eventually forms a broken body; the vertical section of the superposition appears to be separated and flaked, the thickness decreases, the gap increases, etc., and the particles in face-to-face contact are gradually transformed to the edge-to-face contact.

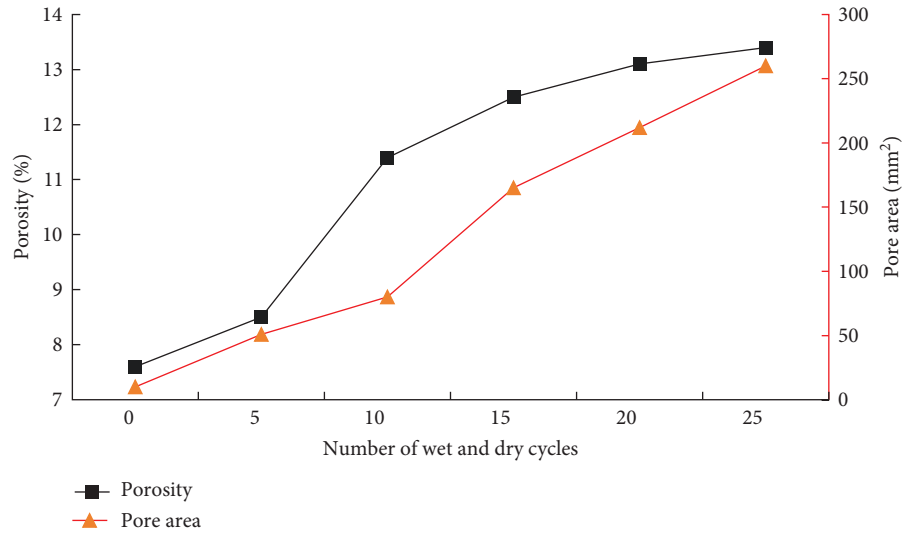


Figure 8: Porosity and pore area variation.

It is evident that the microscopic pore space of the red sandstone increases with the number of wet and dry cycles, resulting in increasingly low tightness between mineral grains and progressively increasing compressibility. The edges of the mineral grains become increasingly rounded and even altered, leading to a gradual deterioration of the overall stability, strength, and deformation properties of the red sandstone. This explains the main reason for the decrease in mechanical properties of red sandstone under the action of wet and dry cycles.

*3.5. Porosity and Pore Area Variation.* In order to further explore the variations in microscopic parameters of red sandstone caused by dry and wet cycles, we employed Image software to analyze the alterations in porosity and pore area under different dry and wet cycles. First set the scale using Image software, convert the image to 8 bit, use the rectangle box selection tool, box in addition to the scale, adjust the threshold, and select the porosity. Calculate the porosity using the measure function of Image software. Porosity = pore area/total area. The findings are presented in Figure 8, which shows a nonlinear rise in porosity and pore area with an increase in the number of dry and wet cycles. At $n = 0$, the porosity and pore area were 7.8% and 25 $mm^2$, respectively. However, at $n = 5$, the porosity and pore area increased to 8.6% and 54 $mm^2$, respectively. The increase in porosity and pore area was more significant when the wet and dry cycle reached 10 times, with a 31.59% and 69.51% increase in porosity and pore area, respectively, compared to 0 dry and wet cycles. This is because the internal microstructure of the red sandstone is less damaged by wet and dry when the number of wet and dry cycles is low. However, when the number of wet and dry cycles is high, fractures and pores within the red sandstone continue to expand, leading to severe damage to the soil structure, weakened intergranular cementation, and longer and wider fissures. At 15 wet and dry cycles, the porosity and pore area increased to 12.6% and 158 $mm^2$, respectively. The maximum porosity and pore area were reached at 25 wet and dry cycles, with a 42.2% and 90.64% increase in porosity and pore area, respectively, compared to 0 wet and dry cycles. The changes in damage variables after wet and dry cycling are the result of the combination of pore enlargement due to damage to the internal red sandstone and the compression of the original fissures. Wet and dry cycling induces damage to the soil structure near the pores and increases the pore size, while wet and dry cycling also contributes to the enlargement of small pores inside the specimen.

*3.6. Study of Damage Laws Based on Fractal Dimension.* The fractal dimension holds great significance in the field of rock mechanics as it serves as an indicator of the complexity of the pore structure of red sandstone. A higher fractal dimension indicates a more intricate pore structure and a greater degree of pore space development. The fractal dimension is calculated using $D = \log(N)/\log(1/r)$, where $D$ is the fractal dimension, $N$ is the number of pixels around each region, and $r$ is the relative size of the region.

Table 3 displays the number of score shape dimensions obtained through Image analysis under varying wet and dry cycles. By applying the principles of fractal damage rock mechanics and calculating the fractal dimension, we can define the damage variable $D_F$ for red sandstone subjected to dry and wet cycling. This variable provides a quantitative measure of the damage inflicted on the red sandstone due to the cyclic exposure to dry and wet conditions:

$$D_F = \frac{\Delta F_{N0}}{F_0} = \frac{F_N - F_0}{F_0} \times 100\%, \quad (3)$$

where $D_F$ is the damage variable, $\Delta F_{N0}$ is the difference between the fractal dimension when $n = 0$. $F_N$ is the fractal dimension, $F_0$ is the fractal dimension in the natural state. This paper focuses on damage to red sandstone by wet and dry cycling and therefore does not consider the initial

Table 3: Fine view damage variables.

| Number of wet and dry cycles | Fractal dimension | Damage variable (%) |
|---|---|---|
| 0 | 1.768 | 0.00 |
| 5 | 1.826 | 3.28 |
| 10 | 1.867 | 5.60 |
| 15 | 1.910 | 8.03 |
| 25 | 1.952 | 10.41 |

damage to red sandstone. Damage variable $D = 0$ for red sandstone in its natural state. The fine view damage variables obtained from Equation (3) are shown in Table 3.

From the data in Table 3, it is clear that the fractal dimension of the red sandstone gradually increases with the number of wet and dry cycles. The structural properties of the pores tend to be more complex, which is consistent with the SEM image findings. The greater the number of wet and dry cycles, the more pronounced the internal microstructural damage to the red sandstone. Quantitative characterization of damage to the fine structure of red sandstone by wet and dry cycling based on damage variables defined by fractal dimension. As the number of wet and dry cycles increases, the damage variable increases, up to 10.41%. It shows that the original pore space and fracture within the red sandstone expand, secondary fracture development evolves, red sandstone damage increases, and dry and wet cycles have effectively increased red sandstone structural damage. The wet and dry cyclic effect tends to induce the expansion of fractures in red sandstone, which leads to a serious impairment of the internal original structure and the cementation between the grains. And the changes in microstructure are the essence of macromechanical changes, further explaining the intrinsic reasons for the decrease in mechanical properties of red sandstone under the action of dry and wet cycles.

## 4. Conclusions

The results of this study demonstrate that red sandstone is significantly affected by wet and dry cycling, resulting in damage degradation. The peak stress in the sandstone was significantly reduced with multiple wet and dry cycles, with a minimum peak stress of 17.30 MPa. Therefore, it is recommended that for geotechnical works or newly exposed slope works, the slopes should be reinforced, taking into account the damage degradation effect of the wet and dry cycle.

Furthermore, the rate of loss of uniaxial compressive strength $\sigma_c$ increased by 46.62% with an increase in the number of repeated wet and dry cycles (25). The loss of modulus of elasticity $E$ reached 49.24%, indicating increasing damage deterioration of the rock by water during the wet and dry cycles.

The porosity and pore area of the red sandstone also increased with the number of wet and dry cycles, with the greatest increase observed after 10 cycles. Additionally, the fractal dimension of the red sandstone gradually increased with an increase in the number of wet and dry cycles. The structural properties of the pores tended to be more complex, which is consistent with the SEM image findings. The injury variable also tended to increase nonlinearly, with a maximum injury variable of 10.41%. With the increase in the number of wet and dry cycles, there was a loss of clay minerals within the specimen, an increase in pore size, a significant increase in microcracks, and a loosening of particle connections.

In summary, the findings of this study highlight the importance of considering the effects of wet and dry cycling on red sandstone in geotechnical and slope works. Future research could focus on developing effective methods for mitigating the damage degradation effect of wet and dry cycling on red sandstone.

## Data Availability

All data used in this study are presented in the manuscript.

## Conflicts of Interest

The authors declare that they have no conflicts of interest.

## Acknowledgments

This work was supported by the Inner Mongolia Natural Science Foundation (Grant No. 2020MS04006), Scientific Research Project of Ordos Institute of Applied Technology (Grant No. KYZD2019002), Scientific Research Project of Academician and Expert Workstation of Mine Geology and Environment, Ordos Institute of Applied Technology (Grant No. 2021 OITYSZJGZZ-008), Ordos Mining Area Geological Disaster Prevention and Geological Environmental Protection Engineering Research Center, the Key Project of Natural Science and Technology of Ordos Institute of Technology (Grant No. KYZD2023004), Scientific Research Project of Academician and Expert Workstation of Mine Geology and Environment, Ordos Institute of Applied Technology (Grant No. 2023 OITYSZJGZZ-004).

## References

[1] X. Song, Y. Hao, J. Huang, S. Wang, and W. Liu, "Study on mechanical properties and destabilization mechanism of unclassified tailings consolidation body under the action of dry–wet cycle," *Construction and Building Materials*, vol. 365, 2023.

[2] J. Tang, H. Sakanakura, A. Takai, and K. Takeshi, "Effect of dry–wet cycles on leaching behavior of recovered soil collected from tsunami deposits containing geogenic arsenic," *Soils and Foundations*, vol. 63, 2023.

[3] J. Jing, J. Hou, W. Sun, G. Chen, Y. Ma, and G. Ji, "Study on influencing factors of unsaturated loess slope stability under

dry–wet cycle conditions," *Journal of Hydrology*, vol. 612, Article ID 128187, 2022.

[4] B. Lian, X. Wang, H. Zhan et al., "Creep mechanical and microstructural insights into the failure mechanism of loesslandslides induced by dry–wet cycles in the Heifangtai platform, China," *Engineering Geology*, vol. 300, Article ID 106589, 2022.

[5] Y. Song, J.-Q. Wang, X.-J. Chen et al., "Study the effects of dry–wet cycles and cadmium pollution on the mechanical properties and microstructure of red clay," *Environmental Pollution*, vol. 302, Article ID 119037, 2022.

[6] P. Wang, J. Xu, X. Fang, M. Wen, G. Zheng, and P. Wang, "Dynamic splitting tensile behaviors of red-sandstone subjected to repeated thermal shocks: deterioration and micro-mechanism," *Engineering Geology*, vol. 223, pp. 1–10, 2017.

[7] Z. Zhou, X. Cai, L. Chen, W. Cao, Y. Zhao, and C. Xiong, "Influence of cyclic wetting and drying on physical and dynamic compressive properties of sandstone," *Engineering Geology*, vol. 220, pp. 1–12, 2017.

[8] Z. Zhou, X. Cai, D. Ma, L. Chen, S. Wang, and L. Tan, "Dynamic tensile properties of sandstone subjected to wetting and drying cycles," *Construction and Building Materials*, vol. 182, pp. 215–232, 2018.

[9] H. Zhang, K. Lu, W. Zhang, D. Li, and G. Yang, "Quantification and acoustic emission characteristics of sandstone damage evolution under dry–wet cycles," *Journal of Building Engineering*, vol. 48, Article ID 103996, 2022.

[10] B. Du, Q. Cheng, L. Miao, J. Wang, and H. Bai, "Experimental study on influence of wetting–drying cycle on dynamic fracture and energy dissipation of red-sandstone," *Journal of Building Engineering*, vol. 44, Article ID 102619, 2021.

[11] W. Yao, C. Li, Q. Ke et al., "Multi-scale deterioration of physical and mechanical properties of argillaceous siltstone under cyclic wetting–drying of Yangtze River water," *Engineering Geology*, vol. 312, Article ID 106925, 2023.

[12] G. Khanlari and Y. Abdilor, "Influence of wet–dry, freeze–thaw, and heat–cool cycles on the physical and mechanical properties of upper red sandstones in central Iran," *Bulletin of Engineering Geology and the Environment*, vol. 74, no. 4, pp. 1287–1300, 2015.

[13] P. Ying, Z. Zhu, L. Ren et al., "Deterioration of dynamic fracture characteristics, tensile strength and elastic modulus of tight sandstone under dry–wet cycles," *Theoretical and Applied Fracture Mechanics*, vol. 109, Article ID 102698, 2020.

[14] X. Cai, Z. Zhou, L. Tan, H. Zang, and Z. Song, "Fracture behavior and damage mechanisms of sandstone subjected to wetting–drying cycles," *Engineering Fracture Mechanics*, vol. 234, Article ID 107109, 2020.

[15] T. Yin, J. Yin, Y. Wu, Z. Yang, X. Liu, and D. Zhuang, "Water saturation effects on the mechanical characteristics and fracture evolution of sandstone containing pre-existing flaws," *Theoretical and Applied Fracture Mechanics*, vol. 122, Article ID 103605, 2022.

[16] Z. Zhou, X. Cai, X. Li, W. Cao, and X. Du, "Dynamic response and energy evolution of sandstone under coupled static–dynamic compression: insights from experimental study into deep rock engineering applications," *Rock Mechanics and Rock Engineering*, vol. 53, pp. 1305–1331, 2020.

[17] W. Xiao, D. Zhang, and X. Wang, "Experimental study on progressive failure process and permeability characteristics of red sandstone under seepage pressure," *Engineering Geology*, vol. 265, Article ID 105406, 2020.

[18] K. Zhao, D. Yang, P. Zeng et al., "Effect of water content on the failure pattern and acoustic emission characteristics of red sandstone," *International Journal of Rock Mechanics and Mining Sciences*, vol. 142, 2021.

[19] B. Zhao, Y. Li, W. Huang et al., "Mechanical characteristics of red sandstone under cyclic wetting and drying," *Environmental Earth Sciences*, vol. 738, 2021.

[20] T. Meng, X. Yongbing, J. Ma et al., "Evolution of permeability and microscopic pore structure of sandstone and its weakening mechanism under coupled thermo-hydro-mechanical environment subjected to real-time high temperature," *Engineering Geology*, vol. 280, 2021.

[21] X. Jiang, C. Li, J.-Q. Zhou et al., "Salt-induced structure damage and permeability enhancement of Three Gorges Reservoir sandstone under wetting–drying cycles," *International Journal of Rock Mechanics and Mining Sciences*, vol. 153, Article ID 105100, 2022.

[22] G. Chen, T. Y. Guo, M. Serati, and B. Pei, "Microcracking mechanisms of cyclic freeze–thaw treated red sandstone: insights from acoustic emission and thin-section analysis," *Construction and Building Materials*, vol. 329, Article ID 127097, 2022.

[23] H. Jiang, A. Jiang, and F. Zhang, "Experimental investigation on damage and seepage of red sandstone subjected to cyclic thermal and cold treatment," *Geoenergy Science and Engineering*, vol. 222, Article ID 211461, 2023.

[24] X. Baoxiang, G. Wenhua, Y. Meihui, Z. Zongtang, and W. Jun, "Analysis of fractal dimension index and influencing factors of red sandstone coarse particle crushing," *Journal of Applied Mechanics*, vol. 6, pp. 1117–1124, 2022.

[25] C. Guanqi, G. Zhaoying, Z. Xiaowen, L. Jian, Z. Zhe, and C. Jiaxin, "Estimation of elastic modulus and decay law of Cenozoic red sandstone based on point load tests," *Journal of Civil Engineering and Management*, vol. 39, no. 6, pp. 71–76, 2022.

[26] G. Wenhua, X. Baoxiang, Y. Meihui, Z. Zongtang, and X. Tianxiang, "Research onthestrength and deformation characteristics of coarse grained red sandstone soil based on large-scale triaxial tests," *Journal of Natural Disasters*, vol. 31, no. 6, pp. 174–180, 2022.

[27] L. Yujie, F. Zhongju, and Z. Yanpeng, "Monitoring and numerical simulation analysis of deep foundation pit support in Lanzhou special red sandstone formation," *Journal of Geotechnical Engineering*, vol. 44, no. S1, pp. 236–240, 2022.

[28] W. Hu, W. Yun, W. Lei, and S. Jinlong, "Experimental study on the degradation of pore structure and tensile strength of red sandstone after high-temperature action," pp. 1–9, Water Resources and Hydropower Technology.

[29] W. Zi, *Research on defect characteristics of red sandstone based on ultrasonic technology*, Xijing University, 2022.

[30] G. Xiaojie, *Analysis of damage deterioration and engineering stability of weakly cemented soft rock under water force coupling*, Shandong University of Science and Technology, 2020.

[31] C. Z. Famous, X. Jinyu, W. Peng, and L. Shaohe, "Static and dynamic splitting tensile tests and microscopic analysis of red sandstone with different water contents," *Journal of Underground Space and Engineering*, vol. 1, pp. 86–92, 2017.

[32] Z. Guanghui, X. Jinyu, W. Peng, L. Shi, and W. Haoyu, "Study on the strain rate effect of red sandstone under water rock coupling cooperation," *Journal of Underground Space and Engineering*, vol. 1, pp. 79–85, 2017.

[33] Z. Guofeng, *Study on true triaxial rock burst test and criterion for water force coupling cooperation*, Chengdu University of Technology, 2016.